J. R. Clark, W.-T. Hsu, and C. T.-C. Nguyen, "Measurement techniques for capacitively-transduced VHF-to-UHF micromechanical resonators" *Digest of Technical Papers*, the 11th Int. Conf. on Solid-State Sensors & Actuators (Transducers'01), Munich, Germany, June 10-14, 2001, pp. 1118-1121.

Measurement Techniques for Capacitively-Transduced VHF-to-UHF Micromechanical Resonators

John R. Clark, Wan-Thai Hsu, and Clark T.-C. Nguyen
Center for Wireless Integrated Microsystems, Dept. of Electrical Eng. and Computer Science
1301 Beal Ave., 2406 EECS Bldg., University of Michigan
Ann Arbor, Michigan 48109-2122 USA
e-mail: jrclark@eecs.umich.edu

ABSTRACT

An electromechanical mixing technique has been demonstrated for accurately measuring the performance of sub-optimal (e.g., insufficiently small capacitive gap, limited dc-bias), high-frequency, high-*Q* micromechanical resonators under conditions where parasitic effects could otherwise mask motional output currents. The technique employs the nonlinear voltage-to-force transfer function inherent in capacitive transducers, allowing an *off-resonance* input signal to mix down to a force at the resonance frequency and drive a resonator into vibration. Using this technique, a *Q* of 9,400 was measured for a non-optimal 156MHz disk resonator—3X higher than the false 3,090 obtained when parasitic feedthrough is allowed to influence the frequency response.

Keywords: disk resonator**,** high-*Q*, test and measurement, RF communications

I. INTRODUCTION

Ongoing frequency extensions of vibrating micromechanical resonators ("μresonators") into the mid-VHF range with *Q*'s approaching 10,000 [1,2,3] have bolstered their position as integrated alternatives to discrete frequency selective components used in reference oscillators and IF filters in wireless systems. In this respect, micromechanical resonators and filters represent a potential enabling technology for fully integrated, RF system-on-a-chip solutions, and with large-scale integration to achieve such functions as RF channel-select filter banks, they are poised to facilitate entirely new transceiver architectures with lower power consumption and greater flexibility [4].

A major challenge with such devices is to design and implement them in such a way that a useful signal can be obtained. Especially in prototype resonators, this problem is compounded by fabrication difficulties such as control of the electrode-to-resonator gap and DC-bias limitations. Such constraints may increase susceptibility to parasitic effects, and for cases where sub-optimal devices invite parasitic interference, obtaining a true measure of device performance requires measurement techniques that can separate the motional current from parasitic effects. This work presents a new measurement technique that accomplishes this goal by driving the resonator with a set of out-of-band signals that are mixed through the transducer nonlinearity [5] to a force component at the resonant frequency. This force drives the resonator and produces an output signal at the resonant frequency, well separated from the input excitation. While this technique is not generally needed in practical applications of μresonators, it is a valuable tool for evaluating early prototype devices, especially for extracting the true *Q*, which is often distorted in the presence of parasitics. For example, a direct transmission measurement of a 156 MHz disk resonator [3] shows a *Q* of only 3,090 due to feedthrough interference. However, using the mixing technique to isolate the motional current yields a more accurate *Q* of 9,400. Whereas previous work focused on the device itself, this work focuses on the measurement techniques crucial to ascertaining the true performance of these devices.

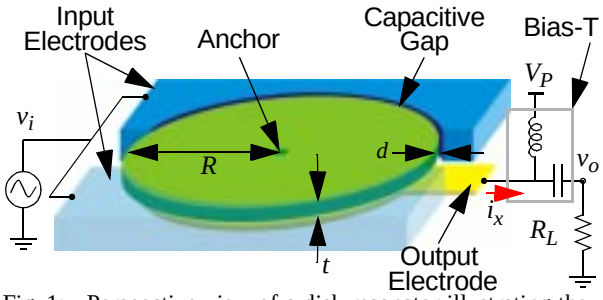

Fig. 1: Perspective view of a disk resonator illustrating the direct measurement (one-port) bias and test scheme.

II. RESONATOR DESIGN AND OPERATION

The measurement techniques described herein were evaluated on the 156 MHz disk resonator depicted in Fig. 1, which identifies key dimensions and shows a one-port bias and excitation scheme. Figure 2 shows an SEM of a disk resonator fabricated using a sub-micron lateral capacitive gap process [8] in order to improve electromechanical coupling. The device consists of a polysilicon disk suspended above the substrate by a single anchor at its center. Input electrodes surround the perimeter of the disk, separated by a narrow vacuum gap. For one-port operation, a DC bias V_P is applied to the structure through a bias-T, while an AC input signal, applied to the electrodes, generates a time-varying, radially-acting force that produces expansion and contraction of the disk along its radius. This motion results in a time-varying DC-biased capacitor generating an output current given by $i_x = V_P(\partial C/\partial x)(\partial x/\partial t)$, where C is the transducer capacitance and x is radial displacement along the disk edge. This motional current can be detected from the structure through a load resistance R_L. The resonant frequency of the disk is inversely proportional to its radius, and vibration in this mode results in a

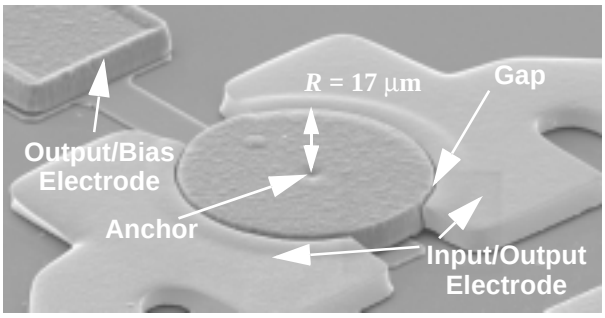

Fig. 2: SEM of a polysilicon disk μresonator fabricated using a lateral sub-micron gap process.

wholly symmetric resonance with a natural nodal point at the center, inherently improving the resonator Q by reducing acoustical energy transfer to the substrate.

III. MEASUREMENT THEORY

Several different approaches to measurement are possible with the disk structure. The following sections present three such techniques and discuss their theory, advantages, and disadvantages.

A. One-Port Measurement

The one-port, direct measurement scheme described in the previous section is the simplest to implement, as it requires only a single input electrode. In this configuration, the equivalent circuit model in Fig. 3(a) represents the resonator, with the series *RLC* components modeling the motional behavior and the capacitor C_o representing the static overlap capacitance between the input electrodes and the structure. At resonance, the admittance of the device is simply given by

$$Y_{in} = \frac{1}{R_x} + j\omega_o C_o \qquad (1)$$

where ω_o is the resonant frequency in radians. For sufficiently large values of C_o relative to R_x, the capacitance term will dominate, resulting in a feed-through current that effectively masks the motional current derived from R_x. Furthermore, C_o creates a parallel-resonance whose frequency is given by

$$f_a = \frac{\sqrt{C_o + C_x}}{2\pi\sqrt{C_o C_x L_x}}. \qquad (2)$$

C_o is typically much larger than C_x, so f_a is often very close to the series resonant frequency $f_o = 1/2\pi\sqrt{C_x L_x}$

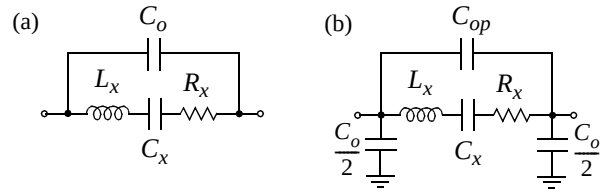

$$L_x = \frac{m_r}{\eta^2} \qquad C_x = \frac{\eta^2}{k_r} \qquad R_x = \frac{\sqrt{k_r m_r}}{Q\eta^2} \qquad \eta = V_P\frac{\partial C}{\partial x}$$

Fig. 3: Equivalent circuit model for (a) one-port measurements; and (b) two-port measurements.

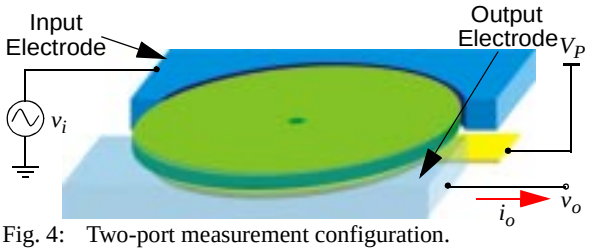

Fig. 4: Two-port measurement configuration.

and can distort the measured signal, shifting the resonant peak, altering the pass band, and making the true performance parameters of the resonator difficult to extract, especially the device Q.

To improve the ratio of C_o to R_x, the electromechanical coupling coefficient η should be increased. According to Fig. 3, this may be accomplished by increasing either V_P or $\partial C/\partial x$, the latter of which is proportional to $1/d^2$ (where d is the electrode-to-resonator gap spacing). V_P is often limited due to pull-in constraints, leaving $\partial C/\partial x$ and thus the gap spacing as the only variable parameter. Hence, in subsequent device generations, the gap can be scaled in order to improve the ratio between R_x and C_o, which is proportional to $1/d^3$. In order to ensure a measurable peak of at least 6 dB, this impedance ratio ($R_x/(1/\omega C_o)$) should be 0.5 or less.

A. Two-Port Measurement

If a second electrode is available, the two-port measurement scheme depicted in Fig. 4 can overcome the problems posed by C_o in a device with sub-optimal gap spacing. In this scheme, the dc bias is applied directly to the structure, while the input electrode is split in half. The ac input signal is applied to one of these electrodes, and the output motional current is detected from the other. With the electrode layout depicted, this excitation scheme results in a non-symmetric force used to excite a symmetric mode shape. However, so long as the force is applied at the frequency corresponding to the symmetric mode, the resultant vibration will assume the correct mode shape with only slight distortion.

Figure 3(b) depicts the equivalent circuit model for the two-port measurement scheme. Here, the static overlap capacitance has been split in half and shunted to ground, and the capacitor C_{op} has been added to model any remaining feedthrough capacitance (e.g., through the substrate). In addition, $\partial C/\partial x$ is reduced by a factor of two because the electrode area has been halved, thus degrading the values of the *RLC* model. However, despite a 4X reduction in output current magnitude, this scheme enables a cleaner measure of resonator performance as the detrimental effects of C_o are now negated by shunting the capacitance to ground.

A. Mixing Measurement

With some device geometries, it may be impractical to fabricate more than one electrode around a resonator, in which case a measurement technique is needed that can separate the motional current from extraneous parasitic currents. One approach to doing this is to excite the

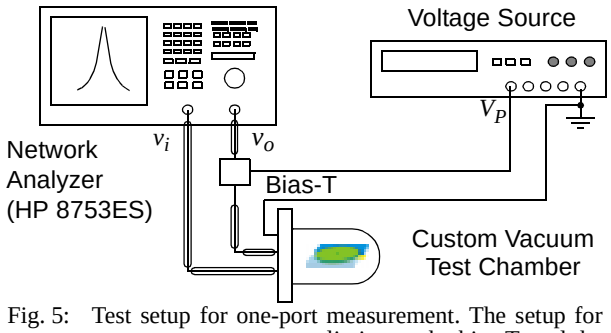

Fig. 5: Test setup for one-port measurement. The setup for two-port measurement eliminates the bias-T, and the dc bias is applied directly to the structure.

resonator with an input frequency different from the resonant frequency [6,7]. Towards this end, the inherent non-linearity of the parallel-plate capacitive transducer may be employed to mix several out-of-band electrical input signals to a force acting at the resonant frequency. This setup is similar to that in Fig. 1, but with an AC excitation v_i given by

$$v_i = V_1\cos\omega_c t + V_2\cos[(\omega_c+\omega_o)t] + V_3\cos[(\omega_c-\omega_o)t] \quad (3)$$

where ω_c is a carrier frequency much higher than ω_o. This input generates a force on the resonator given by

$$F = \frac{1}{2}(V_P - v_i)^2\frac{\partial C}{\partial x} \quad (4)$$

where $\partial C/\partial x$ can be expanded as the Taylor series [5]

$$\frac{\partial C}{\partial x} = \frac{C_o}{d}(1 + A_1x + A_2x^2 + A_3x^3\ldots). \quad (5)$$

Substituting (3) and (5) into (4), results in a series of forces acting at varying frequencies; the most important of which acts at the resonant frequency with a magnitude given by

$$|F_{res}| = \frac{C_oV_1(V_2+V_3)}{2d}. \quad (6)$$

This in-band force is multiplied by the Q of the resonator resulting in vibration at the resonant frequency and output motional current separated from drive parasitics in the frequency domain. Because the inputs are at a much greater frequency than ω_o, they may easily be filtered, resulting in an output current due completely to motion of the resonator with no parasitic effects from C_o.

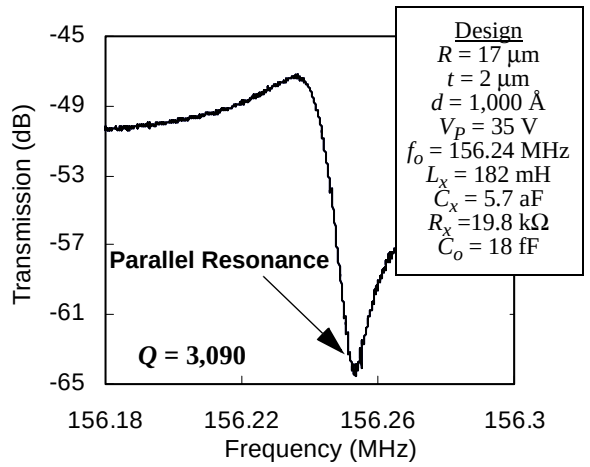

Fig. 6: 156 MHz disk resonator transmission spectrum measured using the one-port setup in Fig. 5.

IV. EXPERIMENTAL SETUP AND MEASUREMENTS

Each of the above measurement techniques were evaluated by applying them to the characterization of a 156 MHz disk resonator at a pressure of 50 µTorr supplied by a custom built vacuum chamber. In comparing the results, particular attention was given to the accuracy of the extracted Q.

A. One and Two-Port Measurements

Figure 5 depicts the test setup for a one-port measurement. Here, the RF-Out port of an HP 8753ES network analyzer is connected directly to the input electrode of the resonator inside the test chamber, and the analyzer's RF-In port is connected to the body of the resonator through a bias-T, as is the bias voltage from a DC power supply. No attempt is made to match the resonator to the testing circuit, as doing so would load the device, reducing its Q. The large mismatch between the 50Ω impedance of the test equipment and the resonator $R_x \sim 20$ kΩ results in a rather high, but tolerable, insertion loss of 47 dB in the measurement.

Figure 6 shows a transmission spectrum obtained from a one-port measurement of a 156 MHz disk resonator along with design parameters and *RLC* element values. Due to the presence of a large C_o, the peak height is less than 4dB above the surrounding feed-through level. The parallel-resonance is also evident as the sharp notch just above the series resonance peak. The combination of these effects leads to an extracted Q of 3,090.

The test setup for the two-port measurement is similar to that of the one-port except that the bias-T is removed, and the dc bias voltage is connected directly to the body of the resonator. The RF-Out port is connected to one half of the metal electrode, and the RF-In port is

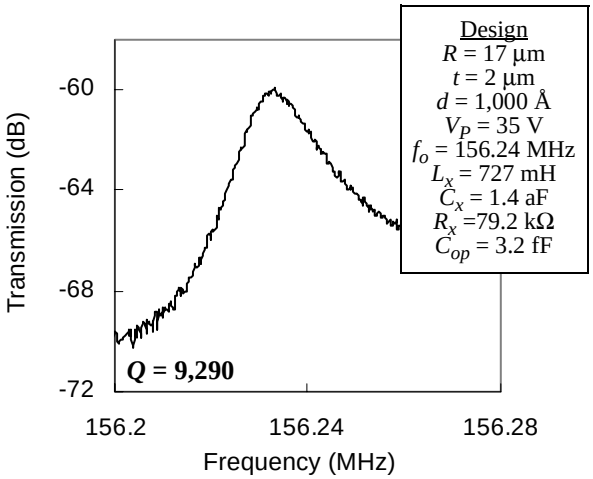

Fig. 7: 156 MHz disk resonator transmission spectrum measured using a two-port setup.

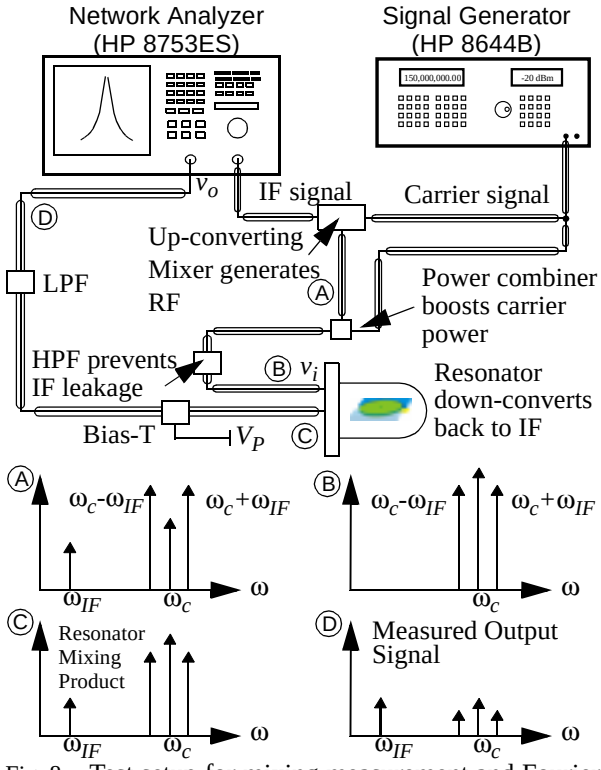

Fig. 8: Test setup for mixing measurement and Fourier spectra at various locations in the setup.

connected to the other. Figure 7 shows a transmission spectrum of a 156MHz resonator obtained via the two-port technique. The insertion loss is approximately 12dB higher, consistent with the 4X increase in R_x and a corresponding 16X decrease in the power measured at the analyzer. However, with reduction of the feed-through capacitance C_o, the peak height has increased to better than 8 dB above the noise floor, while the parallel-resonance has been eliminated. With this more accurate spectrum, the extracted Q is increased to 9,290.

A. Mixing Measurements

Figure 8 depicts the test setup for a mixed measurement. Testing occurs in four steps, outlined in Fig. 8 and denoted by letters in the schematic. First, an IF signal ω_{IF} near the resonant frequency of the device is generated by the network analyzer and mixed via a discrete mixer with a carrier signal ω_c from a signal generator. The resultant Fourier spectrum shown at (A) consists of IF and carrier leakage components and the mixing products. At (B), the input to the resonator, carrier power is re-injected in order to increase signal strength (cf. Eq. (6)), and the IF leakage is blocked by a high pass filter. Non-linearity in the parallel plate capacitive transducer then remixes the carrier and its sidebands, generating a force component acting at the IF frequency that drives the device at resonance and produces the output spectrum at (C). Because the input electrical signal is completely out-of-band, the resultant IF current is entirely derived from the motion of the resonator with no feedthrough interference at ω_{IF}. At (D), the measurement port, a low pass filter blocks feed-through components from the carrier and sidebands to prevent overdriving of the network analyzer. A major advantage of this technique over other mixing techniques [6,7] is that the output signal is at the drive frequency of the network analyzer, allowing direct measurement on the analyzer. Figure 9, obtained from the same resonator as in Fig. 6 but using this mixing technique, shows a peak height greater than 10 dB and a more accurate Q measurement of 9,400 with no signs of parasitic feed-through effects.

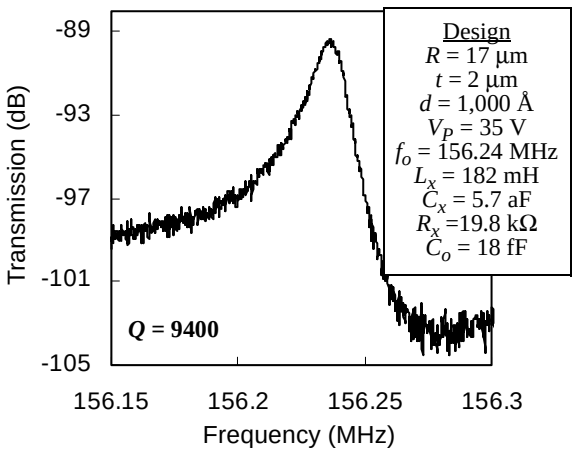

Fig. 9: 156 MHz resonator spectrum obtained using the mixing technique shown in Fig. 8

V. CONCLUSIONS

Several techniques were demonstrated for the accurate characterization of sub-optimal micromechanical resonators under conditions where parasitic currents may mask resonator motional current. Two-port and mixing measurement schemes improved the Q of 3,090 extracted from a one-port measurement to over 9,000 at 156 MHz. While the mixing approach in particular is not required for use in practical applications, such techniques are vital to the rapid evaluation of non-ideal, prototype resonators, as they ease design and fabrication constraints for first generation research devices. Later generations can overcome many parasitic limitations with careful design, and some practical devices such as mechanically coupled filters [9] are inherently two-port, giving them good performance in RF circuits without the need for such complex bias and excitation schemes.

Acknowledgment: This work was supported under DARPA Cooperative Agmt. No. F30602-97-2-0101.

References:

[1] M. Roukes, *Hilton Head 2000*, pp. 367-376.
[2] K. Wang, *et al.*, *MEMS '99*, pp. 453-458.
[3] J. R. Clark, *et al.*, *IEDM 2000*, pp. 493-496.
[4] C. T-C. Nguyen, *BCTM 2000*, pp. 142-149.
[5] R. Navid, *MEMS 2001*, pp. 228-231.
[6] A.-C. Wong, *et al.*, *IEDM '98*, pp. 471-474.
[7] J. Cao, *et al.*, *Transducers '99*, pp. 1826-1829.
[8] W.-T. Hsu, *et al.*, *MEMS 2001*, pp. 349-352.
[9] F. Bannon, *et al.*, *JSSC*, v. 45. n. 4 2000, pp. 512-526.